Chapter 2

Background

The world that we have created thus far creates problems which cannot be solved at the same level we created them

Albert Einstein

2.1 Electrostatic potential as an additional bifurcation variable

Though a seemingly simplistic phenomenon, bubbling involves complex interactions between the gas and the liquid in play. The production of bubbles by various means is used in a plethora of technical applications, especially in the chemical and environmental engineering fields. Water treatment, metallurgy, froth flotation, fermentation, fluidization, and distillation are some widespread examples. Efficient gas-liquid processes introduce the gas in the form of small bubbles, since the greater interfacial area increases interphase heat and mass transfer. In an ideal

gas-liquid system, the bubbles are uniformly sized for even and predictable process performance; however, in reality, gas-liquid systems generally have a broad bubble-size distribution and complex dynamics (Kikuchi & co-workers, 1997; Femat 1998; Luewisutthichat & co-workers, 1997).

Bubble formation in a liquid from a submerged orifice has been the subject of numerous scientific studies, primarily aimed at theoretical prediction and experimental measurement and correlation of bubble size for prediction of interfacial area (Deshpande & co-workers, 1991; Terasaka & co-workers, 1992; Tsuge, 1986; Longuet-Higgins, 1991). Notable among these works is the development of an understanding that bubble size and bubbling frequency is influenced in a complex way on the interactions between consecutively formed bubbles. At low gas flow rates, bubbling is regular and periodic, while at increasing flow rates bubble formation becomes irregular. In their classic paper, Davidson and Schüler (1960) were perhaps the first to illustrate, through high-speed photography, the interaction between leading and trailing bubbles that leads to coalescence at higher flow rates. Subsequently, several investigators have identified different regimes of bubbling, defined by dimensionless groups and characterized by different amounts of interactions between forming bubbles (Miyahara & co-workers, 1984; Tsuge & co-workers 1986). Models for the prediction of bubble volumes have been developed that incorporate the interaction between a primary bubble and subsequent bubbles at higher gas flow rates (Deshpande & co-workers, 1991).

With the availability of the advanced experimental equipment and the advent of the science of nonlinear dynamics, progress has been made recently in the understanding of bubbling. Leighton and co-workers (1990) illustrated the complex hydrodynamic phenomena present in bubbling through both high-speed imaging and acoustic signatures. Chaos in bubbling patterns was

first reported by Tritton and Edgell (1993), who reported a period-doubling bifurcation with gas flow rate in bubbling of air from a single submerged orifice into water-glycerol mixtures. Mittoni and coworkers (1994), reported deterministic chaos in a similar system under a range of conditions by varying chamber volume, injection nozzle diameter, liquid viscosity and gas flow-rate. Similar results were obtained for bubbles by Tufaile & Sartorelli (2000). Nguyen and co-workers (1996), have demonstrated the spatio-temporal behavior of bubbles in single train of rising gas bubbles in a liquid column.

In the above studies, chaotic bubbling was studied primarily with flow rate as the bifurcation variable. Significant effects of external forces on bubbling, such as pulsing a flowing liquid (Fawkner and co-workers, 1988), and application of sound perturbations (Cheng, 1996; Tufaile & Sartorelli, 2000) have been demonstrated. Most notably, Tufaile & Sartorelli (2000) reported the capability to transform a chaotic bubbling state to a periodic state by the application of a synchronized sound wave.

The aim of the present study is to explore whether an applied electrostatic potential can be used as an additional bifurcation variable in bubbling dynamics. If successful, then electrostatic potential can be employed for control.

Zaky and Nossier (1977*)* first reported the effect of an electric field on bubbling, noting a decrease in bubble size and an increase in pressure upstream of the nozzle with increasing voltage for bubbling of air into transformer oil and n-heptane through an electrified needle. Further studies by Ogata et al. (1979, 1985) and Sato et al. (1979, 1980) showed that by the application of a few kilovolts, bubble size can be reduced from a few mm to less than 100 μm in many liquids, including nonpolar fluids like cyclohexane and polar compounds such as ethanol and distilled water. Sato

and coworkers (1993) reported similar results for liquid-liquid systems in which the time scale of electrical charge relaxation (i.e., permittivity/conductivity) of the injected fluid is greater than that of the continuous fluid. This type of dispersion has been termed “inverse electrostatic spraying” (Tsouris et al. 1998) to differentiate it from the well studied “normal” electrostatic spraying (Grace and Marijnissen 1994). Several practical applications have been suggested for this type of spraying, including generating fine bubbles for flow tracers (Sato et al. 1980), enhancing gas-liquid reactions (Tsouris et al. 1995), and producing uniform microcapsules (Sato et al. 1996).

Two main controlling mechanisms have been identified – electric stress and electrohydrodynamic flows. The electric stress acts directly at the gas-liquid interface of growing bubbles and is directed inward (Tsouris et al. 1994; Harris and Basaran 1995). This force is manifested by an increase in nozzle pressure with an increase in applied voltage. Above a critical voltage whose magnitude depends on nozzle geometry, electrohydrodynamic flows are induced in the bulk fluid (Sato et al. 1980, 1993, 1997). These toroidal flows have a significant velocity near the injection nozzle and are directed outward from the points of highest field gradient. Under conditions of electrohydrodynamic flow, a significant decrease in nozzle pressure is exhibited with increasing voltage (Tsouris et al 1998). The dynamics of electrified bubbling are complicated by the interactions of these mechanisms. Sato (1980) described three regimes of bubbling: periodic bubbling, dispersed bubble production, and a high-voltage region characterized by sparking and larger bubble production. Similarly, Shin et al. (1997) outlined three bubbling modes – dripping, an erratic mixed mode, and a spraying mode. These modes were roughly characterized by flow rate using a Reynolds number, and by a combination of electrical forces and buoyancy forces using a modified Weber number. To date, no detailed study of the dynamics of electrified bubbling has

been conducted; for example, it has not been verified that the regimes characterized as periodic are truly periodic, nor are there any detailed analyses and/or means of prediction of the transitions from periodic bubbling. Beyond its intrinsic scientific value, such information would be highly valuable in guiding the production of monodispersed droplets/bubbles.

In the present study, the effect of an applied electrostatic potential on bubbling dynamics was determined experimentally. In these experiments, bubbles were formed in a sufficiently viscous liquid (glycerol) such that electro-hydrodynamic flows were negligible and the main electrostatic mechanism affecting bubbling was the electric stress at the gas-liquid interfaces of the forming bubbles. Deterministic chaos analysis was applied to signals of the temporal fluctuation of pressure in the injection nozzle during bubbling under controlled experimental conditions to probe the combined effect of flow rate and applied voltage on bubble formation dynamics.

2.2 Chaos & feedback control

Identification of electrostatic potential as an additional bifurcation variable provided the basis for further investigation into control of bubbling processes using electrostatic potential as the additional control variable. Study of chaos and understanding the chaotic patterns involved is necessary for implementing control on the bubbling process.

Since the classic paper by Ott, Grebogi and Yorke, (1990) controlling chaos in physical systems has been investigated by many researchers (Ditto & co-workers, 1990,1995; Hunt, 1991; Roy et. al., 1992; Garfinkel & co-workers, 1992; Rollins & co-workers, 1993; Petrov & co-

workers, 1993). This section begins with an introduction to concepts of chaos, and then proceeds to develop the Ott, Grebogi and Yorke, (OGY) control algorithm for a 2-dimensional system (Ditto & co-workers, 1990). A development for multi-variate OGY control is also presented.

2.2.1 Concepts of chaos

Dynamical systems can be represented by equations of motion, which can be written as

$$\dot{x} = F(x, p, t) \tag{1}$$

for continuous systems and

$$\dot{x} = F(x, p, n) \tag{2}$$

for discrete systems. In these equations, we have $x \in \Re^N$, which are state variables, $p \in \Re^{N_p}$, which are system parameters, and $F(\ )$, which is a set of N equations describing the behavior of the system. The solution to equation for continuous systems moves in a N *-dimensional* space called the *phase space* and is usually solved numerically. The basis of this space is given by the state variables x, i.e. the location of the state of the system is determined by taking all the state variables as orthogonal coordinates in the phase space. The system starts out at a certain *initial condition* $x_0 = x(t = 0)$ in space. From the initial condition, dynamical systems trace smooth trajectories in phase space as they proceed in time. The shape in phase space that the trajectory approaches as $t \to \infty$ is called the *attractor* of the system. For periodic motions these trajectories are loops that are traced repeatedly with every period of the system.

Chaos can be termed as the superposition of a very large number of unstable periodic

motions. A chaotic motion may dwell for a brief time on a motion that is very nearly periodic and then may change to another motion that is periodic with a period that is perhaps five times that of the original motion and so on. The constant evolution from one (unstable) periodic motion to another produces a long-term impression of randomness, while showing short-term glimpses of order. (Ditto et al, 1995)

Sensitivity to initial conditions is a hallmark of a chaotic systems. For a chaotic system, there are a very large number of trajectories corresponding to each unstable periodic motion, which pass close together. A small perturbation can shift the system from one trajectory to another. Thus for small changes in the initial state, the subsequent behavior of a chaotic system can appear to be very different.

The phase space trajectories contain all the information necessary to predict the future dynamics of the system. But phase space plots can be complicated and Poincare sections of phase space plots, which are obtained by cutting through the phase space with a plane, are used for simplification (**figure 2.1**). The infinite numbers of points in the phase space are thus reduced and the information contained is more manageable. The number of points in the Poincare section reveals the underlying periodicity of the system. Usually any periodic system of period n has a section, which consists of a finite set of n distinct points, which reflect the fundamental periodicity of the system. However for chaotic systems, the superposition of infinite number of periodic motions causes infinite number of points in the section.

In general the evolution of a chaotic system converges to an extended geometric structure

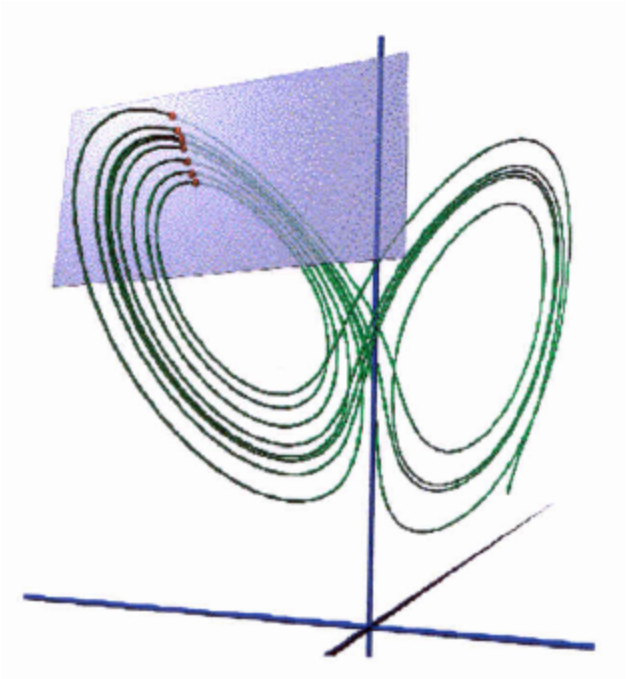

Figure 2.1. Phase space trajectories and the Poincarè section

(Source: Van Goor,1998)

(the chaotic attractor), which is an infinitely long path (implying that it is not periodic motion), but at the same time does not completely fill up the state space, (implying non-random behavior, because a truly random system will have trajectories, which cover the entire volume of phase space available to the system).

In order to control chaos according to the OGY scheme it is only necessary to identify an unstable periodic point in the attractor, to characterize the shape of the attractor locally around that point and to determine the response of the attractor at that point to an external stimulus.

The OGY scheme can replace the Poincare section by a delay coordinate embedding. This embedding depends on the recognition that information obtained by measuring all the system variables (position and momenta) at one given time may also be obtained by only one system variable obtained at several subsequent times. This system state vector (the set of all the positions and momenta, $x_n = (x^1(t_n), x^2(t_n), ..., p^1(t_n), p^2(t_n), ...)$ is replaced by a delay coordinate vector, $(x^i(t_n), x^i(t_n - \Delta t), x^i(t_n - 2\Delta t), x^i(t_n - 3\Delta t), ...)$, where the superscript I indicates on a particular experimental measurable and where Δt is some appropriately chosen delay. In other words the dynamics in full space can be reconstructed from measurements of just one time dependent variable and this time dependent variable carries sufficient information about all the others. For an N degree of freedom system with time series $x(t)$, the signals are plotted versus the delayed or advanced signals by a fixed time constant. The time series generates a trajectory $p(t)$ in N dimensional space.

$$p(t) = \{x(t), x(t + \Delta t), x(t + 2\Delta t), ..., x(t + m\Delta t)\} \quad (3)$$

where m is the embedding dimension and k is the time delay or time lag. According to Takens'

theorem the rule of thumb for selecting time delay of lag involves satisfying the following criteria. $m > 2d + 1$, where d is the actual dimension of the attractor (Takens, 1981). The choice of m and Δt are not crucial except to avoid a natural period of the system.

The OGY control scheme requires the attractor to be characterized and an unstable fixed point on the Poincare section identified, about which control is desired. Then the motion of the point representing the current system state along the stable and unstable directions is identified. The stable and unstable directions on the map are the directions in the neighborhood of the unstable fixed point, in which the current system state is seen to approach and depart to the neighborhood of the fixed point. These two directions form a saddle around the unstable point. These directions *(eigenvectors),* along with the speed *(the eigenvalues),* with which the points approach the fixed point (or depart from the fixed point), characterize the shape of the attractor locally around the fixed point. The OGY control algorithm uses this property of chaotic systems to identify the direction in which control is implemented. These eigenvectors manifest themselves as stable and unstable manifolds on the time return map, which is a low dimension projection of a time delay embedding. On the time return map, the unstable manifold lies along the tangent to the chaotic attractor evaluated at the location of the fixed point.

2.2.2 OGY control

The OGY method waits for the system to land close to the desired fixed point. Once the system is close to the fixed point, the control algorithm perturbs a parameter p such that the next iteration falls onto the stable manifold of the unperturbed system. (**figure 2.2**) The system

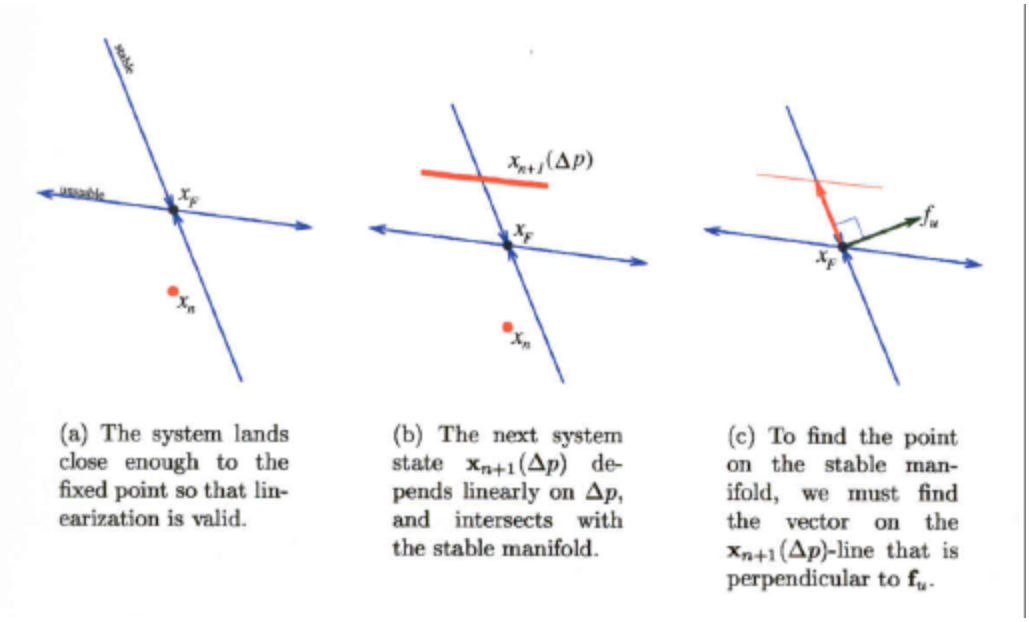

(a) The system lands close enough to the fixed point so that linearization is valid.

(b) The next system state $\mathbf{x}_{n+1}(\Delta p)$ depends linearly on Δp, and intersects with the stable manifold.

(c) To find the point on the stable manifold, we must find the vector on the $\mathbf{x}_{n+1}(\Delta p)$-line that is perpendicular to $\mathbf{f}_u$.

Figure 2.2. OGY control algorithm

(Source: Van Goor,1998)

dynamics will then naturally draw the system closer to the fixed point. The derivation of the OGY algorithm is as follows. The algorithm is based on the linearization of the system close to the location of the fixed point, where the linearization is assumed to be valid. This is a reasonable assumption as the fixed point maps to itself. The linear dynamics can be expressed as:

$$x_{n+1} - x_F(p) = M\left(x_n - x_F(p)\right) \quad (4).$$

where $M \in \Re^{N\times N}$ is the mapping matrix. The mapping matrix M is characterized by its eigenvectors and eigenvalues:

$$\begin{aligned} Me_u &= l_u e_u \\ Me_s &= l_s e_s \end{aligned} \quad (5)$$

where the subscripts u and s correspond to the unstable and stable directions respectively. The eigenvectors are normalized but may be non-orthogonal. The eigenvalues satisfy the condition, $|l_s| < |l_u|$.

Let us consider the space to be two-dimensional. For a two-dimensional map,

$$x = \begin{bmatrix} x_1 \\ x_2 \end{bmatrix} \text{ or } x^T = [x_1 \quad x_2]. \quad (6)$$

In this two-dimensional space there is a map that depends on a parameter p:

$$x_{n+1} = f\left(x_{n,} p\right). \quad (7)$$

The fixed point for this map is also a function of the parameter p:

$$x_F = f\left(x_{F,} p\right). \quad (8)$$

Thus if the parameter is changed every iteration the fixed point also changes:

$$x_F(p_n) = f(x_F(p_n), p\ ). \tag{9}$$

The shift vector s for the estimation of the perturbed fixed point is given by:

$$\begin{aligned} &x_F(p_{n+1}) \sim x_F(p_n) + (p_{n+1} - p_n)s, \\ &s \equiv \frac{d}{dp} x_F(p)\Big|_{p=p_n} \sim \frac{x_F(p_{n+1}) - x_F(p_n)}{p_{n+1} - p_n}. \end{aligned} \tag{10}$$

In the vicinity of the fixed point, the map can be represented by a two dimensional square matrix for two-dimensional space.

$$\begin{aligned} &(x_{n+1} - x_F) \sim M(x_n - x_F), \\ &x_{n+1} \sim x_F + M(x_n - x_F) \end{aligned} \tag{11}$$

If the current state is x_n state of the system after the next iteration depends on the value of the nominal parameter p_o, and the perturbation Δp we apply to it. To find an equation for x_{n+1}, we have,

$$x_{n+1} = x_F(p_o + \Delta p) + M(x_n - x_F(p_o + \Delta p)) \tag{12}$$

Expanding this into a first order Taylor series, we find

$$x_{n+1} = x_F(p_o + \Delta p) + s\Delta p + M(x_n - x_F(p_o) - s\Delta p)) \tag{13}$$

The current state of the system is shown in figure 2.2(a). Equation (13) is shown as a red line in figure 2.2(b). To force the system towards the fixed point, state should be on the stable manifold. To express this condition mathematically, a change of basis is required with the new basis vectors, f_s and f_u defined normal to the unstable and stable manifolds respectively. In the new co-

ordinate system, $(x_{n+1} - x_F)$ has to be orthogonal to the basis vector f_u, (which is in turn orthogonal to the stable direction e_s).

This can be expressed as:

$$f_u^T (x_{n+1} - x_F) = 0 \tag{14}$$

The vectors f_s and f_u can be shown to be the left eigen vectors of M, and are defined as:

$$\begin{aligned} f_u^T M &= l_u f_u^T \\ f_s^T M &= l_s f_s^T \end{aligned} \tag{15}$$

The left and the right eigenvectors are related through the relation

$$\begin{bmatrix} f_u \\ f_s \end{bmatrix}^T = \begin{bmatrix} e_u & e_s \end{bmatrix}^{-1} \tag{16}$$

By replacing $(x_{n+1} - x_F)$ we get

$$0 = f_u^T M \left(x_n - x_F(p) - s\Delta p\right) + f_s^T s\Delta p \tag{17}$$

By replacing M with its eigenvectors

$$0 = l_u f_u^T \left(x_n - x_F(p) - s\Delta p\right) + f_s^T s\Delta p \tag{18}$$

Solving for Δp and substituting $\Delta x_n = x_n - x_F(p)$, we get the OGY formula:

$$\Delta p = \frac{l_u}{l_u - 1} \frac{f_u^T \Delta x_n}{f_u^T s} = c\Delta x_n \tag{19}$$

Comments

The OGY control algorithm is basically a linear model, and it does two things:

1. If the point is on the stable manifold, no action is taken.

2. If the point is not on the stable manifold, it tries to push it onto the stable manifold.

If the final formula is analyzed, it can be explained as the product of a gain, and a ratio of the current direction Δx, of the system to a base case, s. On the numerator, the factor $f_u^T \Delta x$ gives the component of the system along the unstable direction. If the system is orthogonal to the unstable eigenvector and is along the stable eigenvector (assuming a 2-dimension space), and it will map to the fixed point and requires no external perturbation (dot product of orthogonal vectors is zero). After the point proceeds to the unstable direction the control output tries to force it onto the stable manifold and this is possible near the fixed point where the system is at its linear best. As the system goes away from the fixed point, the dot product increases and control output is maximum when the system moves along the unstable manifold trying to force it onto the stable manifold.

The basic assumption of linearity in the OGY control algorithm is that the eigenspace does not change for the system in vicinity of the fixed point. With a small perturbation in the fixed-point location, the stable and unstable manifolds change to orient themselves such that the eigenspace remains the same. This is true for linear systems only, but can be extended to non-linear systems when the change in the eigenspace is not large.

Equation (19) allows for only one system parameter to be controlled because the equation (12) has only one degree of freedom as shown in figure 2.2. The univariate OGY is based on

finding an intersection between the equation for the system state and the stable manifold. For univariate OGY to succeed, there cannot be more than one unstable direction as the control algorithm adjusts the placement of the saddle fixed point through small perturbations of the control variable. Thus, the number of independent control variables needed should be equal to the number of unstable directions. For multi-dimensional spaces, a multi-dimensional return map is plotted and information is extracted for multi-variate control.

Multi parameter OGY

The development of the multivariate OGY control algorithm has been presented by Van Goor, (1998).

Rewriting equation for the system state,

$$x_{n+1} - x_F(p) = S\Delta p + M(x_n - x_F(p_o + \Delta p)) \tag{20}$$

where we now have a N-dimensional system with N_u unstable directions and N_s stable directions, $(N = N_s + N_u)$. In this equation, $\Delta p \in \Re^{N_p = N_s}$ and $S \in \Re^{N = N_u}$ is defined as

$$S = \begin{bmatrix} | & & | \\ \dfrac{\partial x_F}{\partial p_1} & \cdots & \dfrac{\partial x_F}{\partial p_{N_u}} \\ | & & | \end{bmatrix} \tag{21}$$

Thus we have

$$x_{n+1} = Mx_n + (S - MS)\Delta p \tag{22}$$

If x_{n+1} is to be on the stable manifold, then Δx_{n+1} can be expressed as a linear combinations of the

stable eigenvectors of M .

$$x = V_s a \tag{23}$$

where $V_s \in \Re^{N \times N_s}$ and $a \in \Re^{N_s}$

Equating we have,

$$V_s a = M x_n + (S - MS)\Delta p \tag{24}$$

Rearranging,

$$J\Delta x_n = \begin{bmatrix}(S - JS) & V_s\end{bmatrix} \cdot \begin{bmatrix}\Delta p \\ -a\end{bmatrix} \tag{25}$$

Solving for Δp

$$\begin{bmatrix}\Delta p \\ -a\end{bmatrix} = \begin{bmatrix}(S - JS) & V_s\end{bmatrix}^{-1} J\Delta x_n \tag{26}$$

Here only the first N_s elements of the left hand matrix need to be calculated. Δx_n is multiplied with a fixed $N_s \times N$ matrix to obtain the needed parameter perturbations to drive the system into the stable manifold.

2.3 Summary

In this section, the literature survey for bubbling systems was presented. It was noticed that chaos in bubbles has been observed only in the past decade and that attempts to control bubbling concentrated on using flow-rate as the manipulated variable. The effect of electrostatic

potential on bubble/droplet formation has also been reported to be profound, both in terms of the bubble size and frequency. An introduction to chaos and development of a control scheme suggested by Ott, Grebogi & Yorke (1990), has been presented.